Intraband absorption in GaAs-(Ga,Al)As variably spaced semiconductor superlattices under crossed electric and magnetic fields

2013 EPL 104 47008

(http://iopscience.iop.org/0295-5075/104/4/47008)

A Letters Journal Exploring the Frontiers of Physics

November 2013

EPL, **104** (2013) 47008
doi: 10.1209/0295-5075/104/47008

www.epljournal.org

Intraband absorption in GaAs-(Ga,Al)As variably spaced semiconductor superlattices under crossed electric and magnetic fields

E. Reyes-Gómez[1], N. Raigoza[1] and L. E. Oliveira[2]

[1] *Instituto de Física, Facultad de Ciencias Exactas y Naturales, Universidad de Antioquia UdeA Calle 70 No. 52-21, Medellín, Colombia*
[2] *Instituto de Física, Universidade Estadual de Campinas-Unicamp - Campinas, SP, 13083-859, Brazil*

received 8 October 2013; accepted in final form 19 November 2013
published online 16 December 2013

PACS 78.67.-n – Optical properties of low-dimensional, mesoscopic, and nanoscale materials and structures
PACS 78.67.Pt – Multilayers; superlattices; photonic structures; metamaterials
PACS 73.40.Gk – Tunneling

Abstract – A theoretical study of the intraband absorption properties of GaAs-$Ga_{1-x}Al_xAs$ variably spaced semiconductor superlattices under crossed magnetic and electric fields is presented. Calculations are performed for the applied electric field along the growth-axis direction, whereas the magnetic field is considered parallel to the heterostructure layers. By defining a critical electric field so that the heterostructure energy levels are aligned in the absence of the applied magnetic fields, one finds that, in the weak magnetic-field regime, an abrupt red shift of the absorption coefficient maxima is obtained at fields equal to or larger than the critical electric field, a fact which may be explained from the localization properties of the electron wave functions. Results in the strong magnetic-field regime reveal a rich structure on the intraband absorption coefficient which may be explained from the strong dispersion exhibited by both the energy levels and transition strengths as functions of the generalized orbit-center position. Moreover, the possibility of occurrence of absorption in a wide frequency range is also demonstrated. Present calculated results may be of interest for future design and improvement of multilayered-based photovoltaic and solar-cell devices.

In the past few decades, the ability to experimentally realize abrupt-interface semiconductor nanostructures has given a tremendous thrust to the fabrication of physical systems with potential and real applications in a wide variety of optoelectronic devices. In particular, since the pioneering work of Barnham and Duggan [1], the use of semiconductor heterostructures has been increasingly used in the quest for solar cell efficiencies. Variably spaced semiconductor superlattices (VSSLs), a concept proposed by Summers and Brennan [2] for a spaced superlattice in which the well-width variation is chosen so that the electron energy levels are resonant at the operating bias, are specially promising for potential applications in p-i-n solar cells [3–6].

Here we consider a GaAs-$Ga_{1-x}Al_xAs$ VSSL under electric and magnetic fields. The electric field is applied opposite to the growth direction whereas the magnetic field is considered parallel to the layers. The VSSL is constructed by imposing the resonance condition $E^0_{e,n+1} = E^0_{e,n} + e[(a_n + a_{n+1})/2 + b_n]F_c$ between the ground-state energies associated to adjacent wells in the heterostructure, where e is the absolute value of the electron charge, $E^0_{e,n}$ is the ground-state electron energy corresponding to the n-th well of width a_n (assumed as isolated), the width of the n-th barrier is b_n, and F_c is a critical electric field applied perpendicular to the layers so that the heterostructure energy levels are aligned in the absence of magnetic fields. Moreover, we impose the condition $d = a_n + b_n$, with d fixed, and the VSSL may then be generated by using the three parameters, a_1, d, and F_c, as in previous theoretical work [7]. In the present study, we take the VSSL to be composed of N GaAs quantum wells and $N - 1$ interior $Ga_{1-x}Al_xAs$ barriers, with the whole system sandwiched between two semi-infinite $Ga_{1-x}Al_xAs$ barriers.

Therefore, the $2N$ well-barrier interfaces are at the points $y_2, y_3, \ldots, y_{2N+1}$ over the growth axis, with $y_1 \to -\infty$ and $y_{2N+2} \to +\infty$.

Within the effective-mass and parabolic-band approximations, the electron Hamiltonian for a VSSL grown in the y direction is given by

$$\hat{H} = \frac{1}{2m^*}\left(\hat{\vec{\mathbf{p}}} + e\vec{\mathbf{A}}\right)^2 - eF(y - y_c) + V(y), \qquad (1)$$

where V is the VSSL confining potential, the electric field is applied perpendicular to the layers, and y_c denotes the location in which the electrostatic potential energy vanishes. For simplicity we have considered the electron effective mass m^* as constant throughout the heterostructure. We have chosen $\vec{\mathbf{B}} = (0, 0, B)$ and the gauge $\vec{\mathbf{A}} = B(-y, 0, 0)$ for the vector potential. Both x and y are cyclic coordinates in $\hat{H}$, so one may take

$$f_{E,\mathbf{k}_\perp}(\vec{\mathbf{r}}) = \frac{\exp\left[i\vec{\mathbf{k}}_\perp \cdot \vec{\mathbf{r}}_\perp\right]}{2\pi}\varphi_{E,k_x}(y) \qquad (2)$$

as the eigenfunctions of (1), with $\vec{\mathbf{k}}_\perp = (k_x, k_z) = \frac{1}{\hbar}(p_x, p_z)$, $\vec{\mathbf{r}}_\perp = (x, z)$, and p_x and p_z are the eigenvalues of $\hat{p}_x$ and $\hat{p}_z$, respectively. The Landau length and the cyclotron frequency are $l_B = \sqrt{\hbar/(eB)}$ and $\omega_c = eB/m^*$, respectively. One may introduce

$$\phi_{n,\xi_0}(\xi) = \sqrt{l_B}\,\varphi_{E,k_x}(y), \qquad (3)$$

with $\xi = y/l_B$, $\xi_0 = y_0/l_B$, and $y_0 = k_x l_B^2$ as the cyclotron orbit-center position. After a straightforward calculation, one finds that the function ϕ_{n,ξ_0} satisfies

$$\left[-\frac{1}{2}\frac{\mathrm{d}^2}{\mathrm{d}\tau^2} + \frac{1}{2}\tau^2 + v(\xi)\right]\phi_{n,\xi_0}(\tau) = \varepsilon_n(\xi_0 + \xi_{FB})\,\phi_{n,\xi_0}(\tau), \qquad (4)$$

with $\tau = \xi - \xi_0 - \xi_{FB}$, $v(\xi) = V(y)/(\hbar\omega_c)$,

$$\varepsilon_n(\xi_0 + \xi_{FB}) = \epsilon_n(\xi_0, \xi_{FB}) + \xi_{FB}\,(\xi_0 - \xi_c) + \frac{\xi_{FB}^2}{2}, \qquad (5)$$

$$\epsilon_n(\xi_0, \xi_{FB}) = \frac{1}{\hbar\omega_c}\left[E_n(\vec{\mathbf{k}}_\perp) - \frac{\hbar^2 k_z^2}{2m^*}\right], \qquad (6)$$

where $E_n(\vec{\mathbf{k}}_\perp)$ are the eigenvalues of $\hat{H}$, $\xi_{FB} = eFl_B/(\hbar\omega_c) = y_{FB}/l_B$ is the shift of the reduced orbit-center position due to electric-field effects, and $\xi_c = y_c/l_B$. One should note that the eigenvalues of eq. (4) depend on the generalized orbit-center position $\xi_0 + \xi_{FB}$. Equation (4) may be solved by expanding the wave functions ϕ_{n,ξ_0} in a series of the harmonic-oscillator wave functions,

$$h_l(\xi) = \sqrt{\frac{1}{2^l\, l!\,\sqrt{\pi}}}\exp\left[-\frac{\xi^2}{2}\right]\mathrm{H}_l(\xi), \qquad (7)$$

where H_l are the Hermite polynomials, *i.e.*,

$$\phi_{n,\xi_0}(\xi - \xi_0 - \xi_{FB}) = \sum_{l=0}^{+\infty} C_{ln}(\xi_0 + \xi_{FB})\, h_l(\xi - \xi_0 - \xi_{FB}). \qquad (8)$$

Equation (4) may then be transformed into

$$\sum_{l=0}^{+\infty}\left[\left(l + \frac{1}{2}\right)\delta_{kl} + v_{kl}(\xi_0 + \xi_{FB})\right] C_{ln}(\xi_0 + \xi_{FB}) = \varepsilon_n(\xi_0 + \xi_{FB})\, C_{kn}(\xi_0 + \xi_{FB}), \qquad (9)$$

where

$$v_{kl}(\xi_0 + \xi_{FB}) = \int_{-\infty}^{+\infty} h_k^*(\tau)\, v(\tau + \xi_0 + \xi_{FB})\, h_l(\tau)\,\mathrm{d}\tau. \qquad (10)$$

Equation (9) corresponds to a diagonalization problem of a matrix with elements $m_{kl} = (l + 1/2)\delta_{kl} + v_{kl}$ and eigenvalues ε_n. The number M of terms in the sum (8) (and consequently the order of the matrix to diagonalize) may be determined by studying the convergence of the eigenvalues ε_n as functions of M. Results obtained in the present work were computed for $M = 2000$, which guarantees the convergence of the first 100 eigenvalues ε_n up to the fifth decimal place.

The matrix elements v_{kl} of the confining potential may be obtained by setting $\xi_j = y_j/l_B$ as the position of the j-th well-barrier interface in units of the Landau length. In this way one obtains

$$v_{kl}(\xi_0 + \xi_{FB}) = v_0 \sum_{j=1}^{N+1} I_{kl}(\xi_{2j-1} - \xi_0 - \xi_{FB}, \xi_{2j} - \xi_0 - \xi_{FB}), \qquad (11)$$

where v_0 is the height of the confining-potential barriers in units of the cyclotron energy $\hbar\omega_c$ and

$$I_{kl}(a, b) = \int_a^b h_k^*(x)\, h_l(x)\,\mathrm{d}x. \qquad (12)$$

Here we studied the absorption due to transitions of donor electrons between discrete levels of the conduction band. From the experimental point of view, such transitions are usually studied by magnetoabsorption experiments in n-doped GaAs-$Ga_{1-x}Al_xAs$ superlattices, for low doping levels and sufficiently high temperature in order to guarantee the ionization of most of the donor centers. In the Voigt geometry, with the polarization vector $\vec{\boldsymbol{\epsilon}} = \vec{\boldsymbol{e}}_x + \vec{\boldsymbol{e}}_z$ of the normal-incident radiation taken parallel to the x axis, the intraband absorption coefficient may be written as

$$\alpha(\omega) = \frac{2\pi\mu_0 c e^2}{n_R V m^{*2}\omega}\sum_{\mathbf{k}'_\perp,\mathbf{k}_\perp}\sum_{n>m} N_{nm}(\vec{\mathbf{k}}'_\perp, \vec{\mathbf{k}}_\perp) \times\delta\left[E_n(\vec{\mathbf{k}}'_\perp) - E_m(\vec{\mathbf{k}}_\perp) - \hbar\omega\right] \times\left\{\mathcal{F}\left[E_m(\vec{\mathbf{k}}_\perp)\right] - \mathcal{F}\left[E_n(\vec{\mathbf{k}}'_\perp)\right]\right\}, \qquad (13)$$

where μ_0 is the magnetic permeability of the vacuum, n_R is the GaAs refractive index, V is the system volume

$$N_{nm}(\vec{\mathbf{k}}'_\perp, \vec{\mathbf{k}}_\perp) = \left|\vec{\boldsymbol{\epsilon}} \cdot \left\langle f_{n,\mathbf{k}'_\perp}(\vec{\mathbf{r}})\left|\hat{\vec{\mathbf{p}}} + e\vec{\mathbf{A}}\right| f_{m,\mathbf{k}_\perp}(\vec{\mathbf{r}})\right\rangle\right|^2 \qquad (14)$$

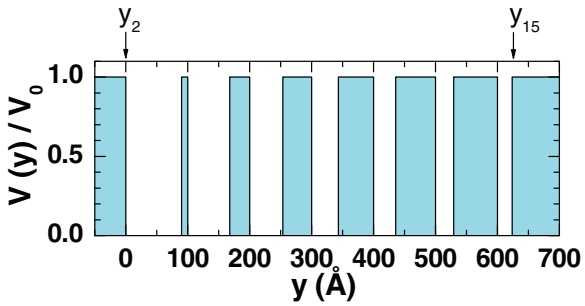

Fig. 1: (Color online) Pictorial view of the variably spaced semiconductor superlattice confining potential with $N = 7$ wells sandwiched between two semi-infinite barriers. The first well width was chosen as $a_1 = 90\,\text{Å}$, and $d = a_n + b_n = 100\,\text{Å}$. The first and last well-barrier interfaces are labeled as y_2 and y_{15}, respectively. Notice that the beginning (end) of the heterostructure is at $y_1 \to -\infty$ ($y_{16} \to +\infty$).

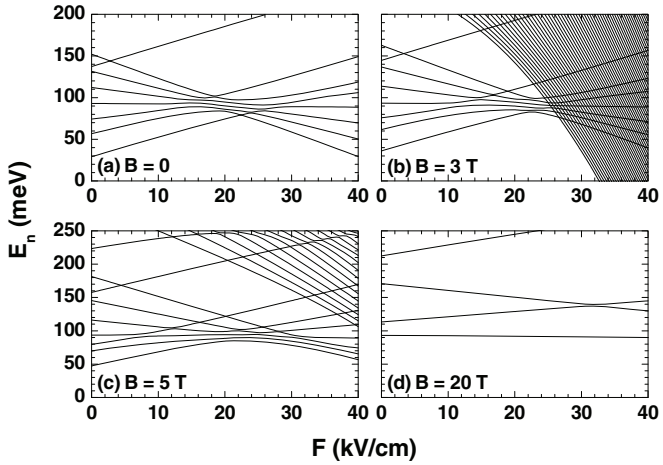

Fig. 2: Electric-field dependence of the conduction-electron energies (E_n eigenvalues of the Hamiltonian (1)) for the GaAs-$Ga_{0.7}Al_{0.3}As$ variably spaced semiconductor superlattice depicted in fig. 1. Calculations were performed for various values of the in-plane magnetic field. The fan diagram displayed in panel (a) was computed through the numerical procedure described in ref. [7]. Numerical results depicted in panels (b)–(d) were obtained (see text) for $k_z = 0$ and the orbit-center position y_0 and y_c taken at the geometrical center of the heterostructure.

is the transition matrix element between the initial state $f_{m,\mathbf{k}_\perp}$ and final state $f_{n,\mathbf{k}'_\perp}$, ω is the incident wave frequency, and $\mathcal{F}$ is the Fermi-Dirac distribution function. Here we note that, for the experimental conditions of low carrier densities and sufficiently high temperature, one may use in eq. (13) the Maxwell-Boltzmann distribution function instead of the Fermi-Dirac one [8]. Moreover, the δ function in eq. (13) may be also replaced by broadened Lorentzian of half-width Γ [8] in order to account for the electron scattering by phonons and impurity centers. We have set $\Gamma = 3\,\text{meV}$ in our theoretical calculations. Equation (14) may be transformed into

$$N_{nm}(\vec{\mathbf{k}}'_\perp, \vec{\mathbf{k}}_\perp) = \frac{e^2 B^2 l_B^2}{2}\, T_{nm}(\xi_0, \xi_{FB})\, \delta\left[\vec{\mathbf{k}}'_\perp - \vec{\mathbf{k}}_\perp\right], \tag{15}$$

where

$$T_{nm}(\xi_0, \xi_{FB}) = 2\,|\langle \phi_{n,\xi_0}(\tau)|\tau|\phi_{m,\xi_0}(\tau)\rangle|^2 \tag{16}$$

is the transition strength normalized to the bulk $0 \to 1$ transition [9].

Here we present the calculated results for the $Ga_{1-x}Al_xAs$-GaAs VSSL depicted in fig. 1, with $N = 7$ wells sandwiched between two semi-infinite barriers. We choose the first well width as $a_1 = 90\,\text{Å}$, and $d = a_n + b_n = 100\,\text{Å}$. The resonant condition for this specific VSSL occurs for $F_c = 20\,\text{kV/cm}$ as the critical electric field. In what follows, we have taken $m^* = 0.067 m_0$ (m_0 is the free-electron mass) and the barrier height of the conduction confining potential as 60% of the band-gap difference $\Delta E_g(\text{eV}) = 1.247x$ between GaAs and $Ga_{1-x}Al_xAs$, where x is the Al concentration in the barriers [7].

We depict in fig. 2 the lowest eigenvalues E_n of the Hamiltonian (1) as functions of the applied electric field. Results shown in fig. 2(a) were obtained in the absence of the applied magnetic field by using the transfer-matrix formalism [7], whereas calculations shown in figs. 2(b), (c), and (d) were computed for in-plane magnetic fields $B = 3\,\text{T}$, $B = 5\,\text{T}$, and $B = 20\,\text{T}$, respectively, for $k_z = 0$ and for both the orbit-center position and y_c taken at the geometrical center of the superlattice. It is apparent from fig. 2(a) that a conduction-electron channel occurs, in the absence of the magnetic field, in the vicinity of the critical electric field. Such channel appears, as expected, because of the electron-resonant tunneling throughout the heterostructure at $F = F_c$. Experimental evidences of the occurrence of such resonant tunneling in VSSL were previously reported [10], a fact which did not receive much attention by the scientific community. It is well known [9] that an applied in-plane magnetic field causes a strong dispersion of the electron energy as a function of the generalized orbit-center position $(\xi_0 + \xi_{FB})$ and, therefore, as a function of the applied electric field via $\xi_{FB} = eFl_B/(\hbar\omega_c)$. Such behavior is clearly observed in figs. 2(b)–(d), where multiple anticrossings take place in the electric-field dependence of the electron energies. One may notice that the shift of the orbit-center position may be rewritten as $\xi_{FB} = \sqrt{2}(\omega_F/\omega_c)^{3/2}$ ($\omega_F = [e^2F^2/(2\hbar m^*)]^{1/3}$ is the electro-optical frequency [7]). It is then apparent that the properties of the electron spectrum are essentially determined by the competition between the electric- and magnetic-field effects. For a given nonzero value of the applied electric field, one may define the weak ($\xi_{FB} \gg 1$) and strong ($\xi_{FB} \ll 1$) magnetic-field regimes.

It is clear from fig. 3, which displays the ground-state electron wave functions for the GaAs-$Ga_{0.7}Al_{0.3}As$ VSSL, that the electron-localization properties of the VSSL are

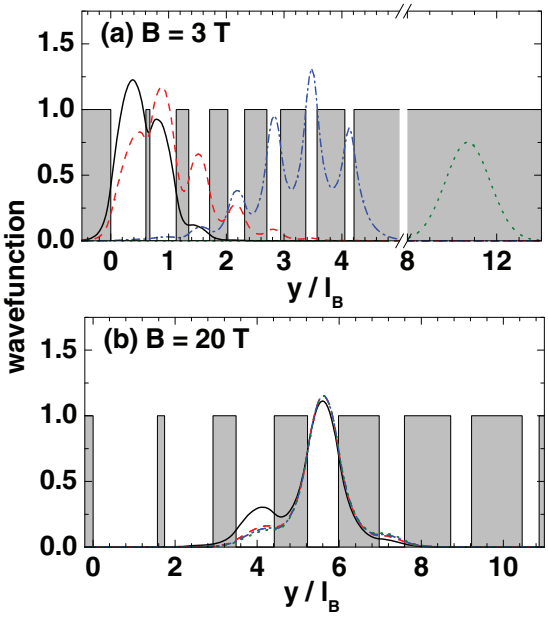

Fig. 3: (Color online) Ground-state electron wave functions for the GaAs-$Ga_{0.7}Al_{0.3}As$ variably spaced semiconductor superlattice of fig. 1. Results were obtained for in-plane magnetic fields of (a) $B = 3\,\mathrm{T}$ and (b) $B = 20\,\mathrm{T}$, $k_z = 0$ and the orbit-center position y_0 and y_c taken at the geometrical center of the heterostructure. Solid, dashed, dot-dashed, and dotted lines correspond to $F = 0$, $F = 20\,\mathrm{kV/cm}$, $F = 25\,\mathrm{kV/cm}$, and $F = 30\,\mathrm{kV/cm}$, respectively.

also determined by the competition between the electric- and magnetic-field intensities. Numerical results in fig. 3 corresponding to solid, dashed, dot-dashed, and dotted lines were obtained for $F = 0$, $F = 20\,\mathrm{kV/cm}$, $F = 25\,\mathrm{kV/cm}$, and $F = 30\,\mathrm{kV/cm}$, respectively, for $k_z = 0$, and for the orbit-center position and y_c taken at the geometrical center of the heterostructure. In the calculations of fig. 3(a) and (b) we have set $B = 3\,\mathrm{T}$ and $B = 20\,\mathrm{T}$, respectively. One may note from fig. 3(a), for $F \neq 0$, that in the weak magnetic-field regime the localization properties of the electron wave functions are governed by the intensity of the applied electric field. As in this regime $\xi_{FB} \gg 1$, the $\xi_0 + \xi_{FB}$ generalized orbit-center position strongly depends on the electric field. As the electron wave function is localized around $\xi_0 + \xi_{FB}$, one may note that such localization center may be dramatically modified as the electric field changes. For electric-field intensities in the vicinity of the critical field F_c, it is possible to observe the spreading of the wave function over a wide region of the superlattice, a fact which is due to the occurrence of the resonant tunneling through the heterostructure. If the electric-field intensity is larger than the critical field, then the electron wave function localizes deep inside the right $Ga_{0.7}Al_{0.3}As$ barrier (see dotted line in fig. 3(a)), a physical situation which corresponds to an electron "escaping" from the heterostructure in the direction opposite to the applied electric field. In the strong magnetic-field regime, one has $\xi_{FB} \ll 1$ and, therefore, the $\xi_0 + \xi_{FB}$ localization center of the electron wave functions is weakly dependent on the electric-field intensity. In this case the magnetic field tends to localize the electron wave functions around the ξ_0 cyclotron orbit-center position for the all values of the electric field considered in the present study. Such physical situation may be observed in fig. 3(b).

In order to study the intraband absorption properties of the VSSL, it is of crucial importance to compute the reduced energies ε_n by appropriately solving eq. (4). It is possible to show [9] that the reduced energies are connected with the matrix elements of the transition strength by the sum rule

$$\sum_{n=0}^{+\infty} \left[\varepsilon_n(\xi_0 + \xi_{FB}) - \varepsilon_m(\xi_0 + \xi_{FB})\right] T_{nm}(\xi_0, \xi_{FB}) = 1. \tag{17}$$

A calculation (results not shown here) of the transition energies $\Delta\varepsilon_n = \varepsilon_{n+1} - \varepsilon_n$ and the intraband transition strengths $T_{n+1,n}$, corresponding to some $n \to n+1$ transitions between consecutive energy levels, indicates that, for a given value of n, $\Delta\varepsilon_n$ behaves in the oppositive way to its associated transition strengths $T_{n+1,n}$ as a function of the generalized orbit-center position. This may be understood from eq. (17) by taking into account that $T_{n+1,n} \gg T_{n+k,n}$, with $n \geq 0$ and $k > 1$.

We now turn to fig. 4, where we display the intraband absorption coefficient, as a function of the incident-wave frequency ω, corresponding to the GaAs-$Ga_{0.7}Al_{0.3}As$ VSSL of fig. 1, at a given temperature. Results were computed for in-plane magnetic fields $B = 3\,\mathrm{T}$ and $B = 20\,\mathrm{T}$, and for two different values of the temperature. Solid, dashed, dot-dashed, and dotted lines in all panels of fig. 4 correspond to applied electric fields $F = 0$, $F = 10\,\mathrm{kV/cm}$, $F = 20\,\mathrm{kV/cm}$, and $F = 30\,\mathrm{kV/cm}$, respectively. The overall behavior of the intraband absorption coefficient as a function of ω may be quantitatively understood in terms of the electronic structure and localization properties of the electron states. In the weak magnetic-field regime and for $F < F_c$ electric-field intensities, the $\alpha(\omega)$ absorption coefficient essentially has peaks at the frequency regions corresponding to absolute maxima and minima of $\Delta\varepsilon_n$ (cf. figs. 4(a) and (b)). In contrast, for the $F = F_c$ electric-field intensity, the electron wave functions spread over the entire superlattice, whereas if $F > F_c$ the wave functions tend to localize in a $Ga_{0.7}Al_{0.3}As$ barrier, as explained before. Under such circumstances, the intraband absorption behaves in a similar way to the absorption due to the bulk-cyclotron resonance, and the absorption coefficient peaks around the cyclotron frequency ω_c (cf. the insets of figs. 4(a) and (b)). Therefore, an abrupt red shift of the intraband absorption peaks is expected to occur at the critical electric field in the weak magnetic-field regime. On the other hand, in the strong magnetic-field regime, the intraband absorption coefficient exhibits a rich structure due to the strong dispersive character of the energy levels and transition

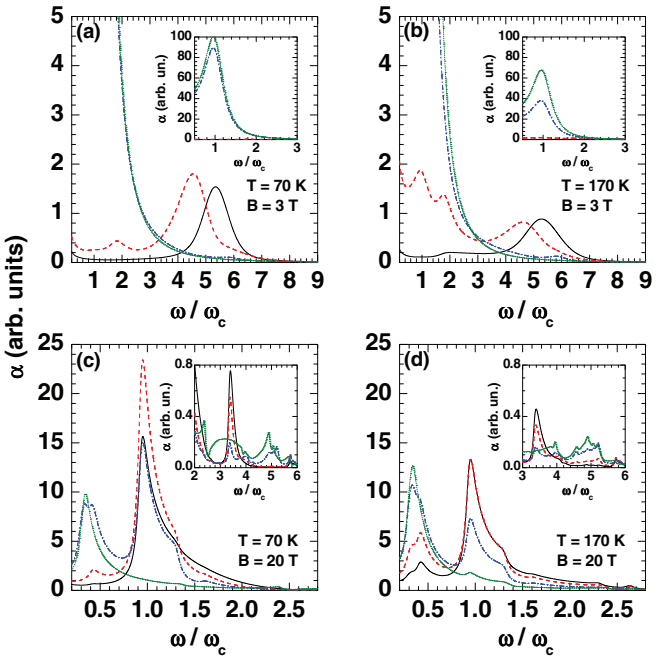

Fig. 4: (Color online) Intraband absorption coefficients for the variably spaced GaAs-$Ga_{0.7}Al_{0.3}As$ semiconductor superlattice of fig. 1. Results shown in panels (a) and (b) correspond to an in-plane magnetic field of $B = 3\,\mathrm{T}$, whereas $B = 20\,\mathrm{T}$ in panels (c) and (d). Numerical calculations were performed for two different values of the temperature. Solid, dashed, dot-dashed, and dotted lines correspond to applied electric fields $F = 0$, $F = 10\,\mathrm{kV/cm}$, $F = 20\,\mathrm{kV/cm}$, and $F = 30\,\mathrm{kV/cm}$, respectively.

strengths as functions of the generalized orbit-center position. Although most of the intraband absorption takes place in the vicinity of the cyclotron frequency, absorption also occurs up to $\omega \sim 6\omega_c$, as one may note from figs. 4(c) and (d), and corresponding insets. It is important to stress that a variation in the system temperature does not dramatically modify the properties of the intraband absorption coefficient in all cases discussed above.

Summing up, we have investigated the intraband absorption properties of GaAs-$Ga_{1-x}Al_xAs$ VSSLs under crossed magnetic and electric fields. The applied electric field was taken in the oppositive direction to the growth axis, whereas the magnetic field was considered to be parallel to the heterostructure layers. Both the weak and strong magnetic-field regimes were analyzed for a given nonzero value of the applied electric field. For each regime, different electronic structures, electron-localization, and intraband absorption coefficient properties were discussed. In the weak magnetic-field regime, an abrupt red shift of the absorption coefficient maxima were observed at the critical electric field, a fact which was explained from the localization properties of the electron wave functions for electric fields larger than F_c. In the strong magnetic-field regime, a rich structure on the intraband absorption coefficient was observed and explained from the strong dispersion exhibited by both the energy levels and transition strengths as functions of the generalized orbit-center position. In addition, the possibility of occurrence of absorption in a wide frequency band (up to $\omega \sim 6\omega_c$) was also shown. In conclusion, we have demonstrated that, by appropriately choosing VSSL geometrical parameters, applied electric and magnetic fields, as well as temperature effects, one may modify the spectral and resonant-tunneling responses, allowing for the possibility of suitable device applications. More specifically, the present theoretical results may be of importance for future design and improvement of multilayered-based photovoltaic and solar-cell devices.

* * *

ER-G wishes to acknowledge the warm hospitality of the Institute of Physics of the Universidade Estadual de Campinas, where part of this work was performed. We are grateful to the Scientific Colombian Agency CODI - University of Antioquia and Brazilian Agencies CNPq, FAPESP (Proc. 2012/51691-0), and FAEPEX-UNICAMP, for partial financial support.

REFERENCES

[1] Barnham K. W. J. and Duggan C., *J. Appl. Phys.*, **67** (1990) 3490.
[2] Summers C. J. and Brennan K. F., *Appl. Phys. Lett.*, **48** (1986) 806; **51** (1987) 276; Brennan K. F. and Summers C. J., *J. Appl. Phys.*, **61** (1987) 5410; 614.
[3] Courel M., Rimada J. C. and Hernández L., *Appl. Phys. Lett.*, **100** (2012) 073508.
[4] Courel M., Rimada J. C. and Hernández L., *J. Appl. Phys.*, **112** (2012) 054511.
[5] Cabrera I., Rimada J. C., Connolly J. P. and Hernández L., *J. Appl. Phys.*, **113** (2013) 024512.
[6] Jo M., Ding Y., Noda T., Mano T., Sakuma Y., Sakoda K., Ham L. and Sakaki H., *Appl. Phys. Lett.*, **103** (2013) 061118.
[7] Reyes-Gómez E., Oliveira L. E. and de Dios-Leyva M., *Physica B*, **358** (2005) 269.
[8] de Dios-Leyva M., Bruno-Alfonso A. and Oliveira L. E., *J. Phys.: Condens. Matter*, **9** (1997) 1005.
[9] de Dios-Leyva M., Bruno-Alfonso A., Reyes-Gómez E. and Oliveira L. E., *J. Phys.: Condens. Matter*, **7** (1995) 9799.
[10] Cao S. M., Willander M., Ivchenko E. L., Nesvizhskii A. I. and Toropov A. A., *Superlattices Microstruct.*, **17** (1995) 97; Cao S. M., Willander M., Toropov A. A., Shubina T. V., Ya. Mel'tser B., Shaposhnikov S. V., Ko'pev P. S., Holt P. O., Bergman J. P. and Monemar B., *Phys. Rev. B*, **51** (1995) 17267.